

# GENERATION OF NANOCOMPOSITES BASED ON (PMMA-*b*-PCL)-GRAFTED Fe<sub>2</sub>O<sub>3</sub> NANOPARTICLES AND PS-*b*-PCL BLOCK COPOLYMER

Irati Barandiaran<sup>1</sup>, Ariel Cappelletti<sup>2</sup>, Miriam Strumia<sup>2</sup>, Galder Kortaberria<sup>1\*</sup>

<sup>1</sup> “Materials + Technologies” Group, Universidad del País Vasco/Euskal Herriko Unibertsitatea, Plaza Europa 1, 20018 Donostia, Spain

<sup>2</sup> Facultad de Ciencias Químicas, Universidad de Córdoba, Haya de la Torre Esq. Medina Allende 5000, Córdoba, Argentina

## ABSTRACT

The aim of this work is to obtain a good dispersion of Fe<sub>2</sub>O<sub>3</sub> magnetic nanoparticles into a PS-*b*-PCL diblock copolymer. For this purpose nanoparticles have been modified in their surface by grafting a PMMA-*b*-PCL block copolymer into their surface, after being silanized. The grafting process has been probed by infrared spectroscopy, thermogravimetric analysis and transmission electron microscopy. Once modified, nanoparticles have been dispersed into the block copolymer. Nanostructured lamellar morphology of the block copolymer after annealing process has not been affected by the presence of nanoparticles, as has been probed by atomic force microscopy. Furthermore, their dispersion into the matrix has been improved when compared with unmodified nanoparticles. Though during modification process small aggregates of nanoparticles surrounded by PMMA-*b*-PCL brushes have been formed, morphology has not been altered or disrupted. Modified nanoparticles have been mostly placed at the interfaces among PS and PCL domains.

## 1. INTRODUCTION

Self-assembly of block copolymers can generate a rich variety of nanostructures depending on the nature of the blocks, molecular weight and composition, and processing characteristics. Microphase or nanophase separation at the mesoscopic scale is generated by the repulsion between blocks linked by covalent attachment. This materials could open a way to generate different nanostructures with applications in fields such as medicine [1], surfactant chemistry [2], quantum dots [3], microcapsules [4], nanowires [5] and magnetic storage media [6, 7], among others. In that way, the incorporation of inorganic nanoparticles into nanophase-separated structures could enable to obtain nanocomposites with prominent features such as optic, electronic, and magnetic properties [8-10].

On the other hand, magnetic nanoparticles have received special attention due to its potential applications in many diverse fields such as ferrofluids, magnetic resonance imaging, biomedicine, drug delivery, etc [11-14].

The control of nanoparticle dispersion and their placement into desired domains is the main goal of preparing nanocomposites based on block copolymers and nanoparticles that tend to form big aggregates. In order to overcome this problem, the use of surfactants [15] or functionalization of nanoparticle surface with polymeric brushes are the most common routes [11, 16]. Different methods have been used for anchoring polymeric brushes in the surface of nanoparticles, such as *grafting to* [17], *grafting from* [11] or *grafting through* [18]. In the first method end-functionalized polymer reacts with the reactive sites on nanoparticle surface. In the *grafting from* method the polymer chains grow in situ from an initiator that has been previously anchored to nanoparticle surface. The last method consists on a surface copolymerization through a covalently linked monomer in which the inorganic phase is incorporated inside polymer chains.

Functionalization of magnetic nanoparticles surface with copolymers is becoming an extended practice. In this way, Wang et al. [19] functionalized iron oxide nanoparticles with P(PEGMA)-*co*-PNIPAAm copolymer via surface charge transfer free radical polymerization, Zhou et al. [20] functionalized magnetic nanoparticles with PEGMA-*b*-PMMA via atom transfer radical polymerization (ATRP), while He et al. [21] functionalized magnetic nanoparticles with a novel water soluble triblock copolymer via copper mediated atom transfer radical polymerization.

In this work, Fe<sub>2</sub>O<sub>3</sub> magnetic nanoparticles have been functionalized by grafting a poly(methyl methacrylate-*b*- $\epsilon$ -caprolactone) (PMMA-*b*-PCL) copolymer to their surface in order to better disperse them into a poly(styrene-*b*-caprolactone) (PS-*b*-PCL) block copolymer without breaking nanostructures generated by thermal annealing.

## **2. EXPERIMENTAL**

### **2.1. Materials**

Maghemite (Fe<sub>2</sub>O<sub>3</sub>) nanoparticles with a nominal size of 9 nm and a polydispersity of 1.08 were purchased from Integram Technologies. 3-aminopropyltriethoxysilane (APTS) was purchased from Sigma-Aldrich, with a purity of 99 %. Poly(methyl

methacrylate-*b*- $\epsilon$ -caprolactone) block copolymer with terminal chlorine group (*Cl*-PMMA-*b*-PCL) was synthesized by ATRP with a molecular weight per number of 21,500 g/mol ( $f_{PMMA} = 0.7$  and  $f_{PCL} = 0.3$ ) and a polydispersity of 1.35. Poly(styrene-*b*- $\epsilon$ -caprolactone) (PS-*b*-PCL) block copolymer ( $f_{PS} = 0.7$  and  $f_{PCL} = 0.3$ ) was purchased from Polymer Source, Inc.. The molecular weights ( $M_n$ ) of PS and PCL blocks are 27,000 and 10,000 g/mol, respectively, with a polydispersity index of 1.25. Toluene and tetrahydrofuran purchased from Aldrich were used as solvents.

## 2.2. Nanoparticle modification

Nanoparticle modification was carried out in two steps: first silanization process and then PMMA-*b*-PCL copolymer grafting to the silanized surface.

### 2.2.1. Silanization process

Fe<sub>2</sub>O<sub>3</sub> magnetic nanoparticles were first modified with 3-aminopropyltriethoxysilane (APTS). Scheme 1 shows the reaction of nanoparticles with silane. This reaction implies a nucleophilic attack of OH groups at nanoparticle surface to the Si atoms of APTS. Extradry toluene, APTS and nanoparticles were mixed under sonication at inert atmosphere for 3 h at room temperature. Nanoparticles were subsequently washed six times with THF and then dried *in vacuo* at 40 °C for a period of 2 days. 1:1, 1:2, 1:3 and 1:5 OH/APTS molar ratios were investigated and as the highest silane grafting density was obtained for 1:3 ratio (as it will be shown below with TGA measurements), nanoparticles modified with this ratio were subsequently used for copolymer grafting.

### 2.2.2. Grafting to process

The anchoring of block copolymer was done by *grafting to* method. The covalent linking among silanized nanoparticles and PMMA-*b*-PCL block copolymer (with terminal *Cl*-group) was carried out by an alkylation reaction of amine groups present at the surface of nanoparticles, as it can be seen in Scheme 2. Extradry toluene solution of silanized nanoparticles and block copolymer was prepared. Grafting reaction was carried out at room temperature for 6 h with reflux. Functionalized nanoparticles were then cleaned six times with THF by centrifugation and then dried *in vacuo* at room temperature for a period of two days. 8, 11, 15 and 22 % copolymer/APTS molar ratios were investigated. The

highest grafting density was obtained for 15 %, as it will be shown below with TGA measurements.

### **2.3. PS-*b*-PCL/Fe<sub>2</sub>O<sub>3</sub>-*g*-(PMMA-*b*-PCL) nanocomposite preparation**

Fe<sub>2</sub>O<sub>3</sub>-*g*-(PMMA-*b*-PCL) nanoparticles were first dispersed in toluene for 2 h by sonication. Then PS-*b*-PCL block copolymer was added to the solution and films were prepared by spin coating. Obtained films were annealed at different temperatures under vacuum, together with those films of block copolymer without nanoparticles, prepared under the same conditions. Nanocomposites with 2 and 5 wt% of nanoparticles were prepared. The effect of annealing temperature, nanoparticle addition and concentration will be analyzed.

### **2.4. Characterization techniques**

Brunauer-Emmet-Teller (BET) isotherms were obtained with an Autosorb-1 from Quantachrome. Samples were dried at 100 °C for 2 h in a vacuum oven. Nitrogen was used as the adsorbent, and all measurements took place at -196 °C.

Fourier transformed infrared spectroscopy (FTIR) was carried out with a Nicolet Nexus 600 FTIR spectrometer, performing 20 scans for each sample with a resolution of 4 cm<sup>-1</sup>.

Thermogravimetric analysis was performed with a Mettler Toledo TGA/SDTA851 instrument. Tests were carried out from room temperature to 750 °C with a heating rate of 10 °C/min.

Nanoparticle size after modification was analyzed by transmission electron microscopy (TEM). A solution drop was deposited on a Formvar film Copper grid and examined in a Tecnai G2 20 Twin (FEI) microscope operating at an accelerating voltage of 200 keV in a bright-field image mode.

Morphologies obtained for different films were studied by atomic force microscopy by a scanning probe microscopy AFM Dimension ICON of Bruker, operating in tapping mode (TM-AFM). An integrated silicon tip/cantilever, from the same manufacturer, having a resonance frequency of around 300 kHz, was used. Measurements were performed at a scan rate of 1 Hz/s, with 512 scan lines.

### 3. RESULTS AND DISCUSSION

#### 3.1. Fe<sub>2</sub>O<sub>3</sub> nanoparticle characterization

The specific surface area of the nanoparticles measured with the BET method was estimated to be 102 m<sup>2</sup>/g. The quantity of hydroxyl groups on the surface was determined with the use of TGA according to the method of Abboud et al [22]. The surface density of hydroxyl groups was found to be 5.5 OH/nm<sup>2</sup>. A typical FTIR spectrum of nanoparticles is shown in Figure 1. The peak around 3400 cm<sup>-1</sup> can be attributed to O-H bonds of nanoparticle hydroxyl groups. The other two peaks at 633 and 558 cm<sup>-1</sup> are due to the Fe-O bond [23, 24]. As it can be seen, there is a complete absence of any carbon-related peaks, this showing that nanoparticles were surfactant-free.

#### 3.2. Fe<sub>2</sub>O<sub>3</sub> nanoparticle silanization

The introduction of APTS onto nanoparticles is of crucial importance for further grafting of PMMA-*b*-PCL to the surface by the amino groups of silane. After modification, the amount of grafted silane was determined by TGA [25]. The surface density of the silane was about 1.9 molecules/nm<sup>2</sup>. A direct comparison of the surface density of hydroxyl groups and that of the silane on the surface yielded a reaction efficiency of 35.8%. Those data were measured for nanoparticles modified with 1:3 OH/APTS molar ratio, which gave the highest silane density and efficiency. For this reason, 1:3 ratio was chosen for nanoparticle silanization. The reaction between the hydroxyl groups and APTS was confirmed by FTIR. Figure 1 shows FTIR spectrum of silanized nanoparticles together with that corresponding to pristine nanoparticles. Characteristic absorption bands of the aminopropyl groups, as well as the stretching vibration of Fe-O and Si-O bonds can be seen, together with the bands related to aliphatic C-H bonds [26]. The presence of the peak related with O-H bonds seems to indicate that not all hydroxyl groups have reacted, as was determined by TGA. These experimental findings strongly suggest that APTS indeed reacted with the surface OH groups.

#### 3.3. PMMA-*b*-PCL grafting

Figure 2 shows FTIR spectra of nanoparticles grafted with PMMA-*b*-PCL copolymer. As it can be seen, the presence of the band related to the stretching vibrations of carbonyl group and that corresponding to COC single bond stretching deformation vibration,

present in both PMMA and PCL blocks, suggest that copolymer has been grafted to the silanized nanoparticle surface. Figure 3 shows the weight loss of unmodified, silanized and copolymer-anchored Fe<sub>2</sub>O<sub>3</sub> nanoparticles, as obtained from TGA measurements. The weight loss of unmodified nanoparticles is related to physisorbed water (between 25-150 °C) and surface –OH degradation (between 150-850 °C) [27]. For silanized nanoparticles, a significant weight loss starts at around 300 °C, related with silane aminopropyl group decomposition [26, 28], that was used for the determination of APTS surface density. When the copolymer is anchored to the nanoparticle, different weight loss steps are observed. Besides silane decomposition, thermal decomposition of copolymer can be seen: the decomposition of PCL block occurs in a single step between 200 and 350 °C [29], while main thermal decomposition for PMMA occurs at around 400 and 600 °C [30]. Besides confirming copolymer anchorage, TGA measurements were used to quantify the grafting density of PMMA-*b*-PCL anchored to nanoparticles with the method proposed by Ohno et al [31]. The highest graft density (0.04 chains/nm<sup>2</sup>) was found for 15% copolymer/APTS molar ratio, while the rest of molar ratios used gave lower densities. At this step reaction yield is of around 2 %. Nanoparticles with 0.04 chains/nm<sup>2</sup> grafting density were used for nanocomposite preparation.

TEM measurements were also used for nanoparticle characterization before and after modification reactions. Figure 4 shows TEM images of both unmodified and copolymer-grafted nanoparticles. It can be seen that during grafting process nanoparticles tend to aggregate and the modification does not occur around a single nanoparticle but around small aggregates, around which the copolymer can be seen in Figure 4b. The average size of aggregates is between 20 and 40 nm.

### **PS-*b*-PCL/Fe<sub>2</sub>O<sub>3</sub>-*g*-(PMMA-*b*-PCL) nanocomposite characterization**

Morphologies obtained for both copolymer and nanocomposites thin films annealed at 100 and 120 °C have been analyzed by AFM. Figure 5 shows AFM images of neat block copolymer films annealed at 100 and 120 °C for 72 h. Films annealed at 100 °C (figure 5a) show worm-like morphology, in which bright domains correspond to PS block, as it is the hardest phase. When annealing temperature is 120 °C (figure 5b) a lamellar morphology can be clearly seen. It is worth to note that PCL crystalline domains are not observed in the images. In fact, as it was measured by differential scanning calorimetry (not shown here), crystallization degree of PCL block (only 30% of copolymer) was

below 5% in both cases. Furthermore, for nanocomposites crystallization degrees are even lower than 1%.

Figure 6 shows AFM images of nanocomposites with 2 and 5 wt% of nanoparticles annealed at 100 and 120 °C. As it can be seen the addition of Fe<sub>2</sub>O<sub>3</sub> nanoparticles does not modify the morphology of block copolymer. Samples annealed at 100 °C present a worm-like morphology very similar to that of neat copolymer, while those annealed at 120 °C present nanostructured lamellar morphology similarly to neat copolymer. Bright points observed in images of Figure 6 can be attributed to Fe<sub>2</sub>O<sub>3</sub> nanoparticles; the amount of points obviously increases with nanoparticle content. Although small nanoparticle aggregates were formed during grafting process, functionalized nanoparticles are well dispersed in the copolymer. The grafting of nanoparticles with PMMA-*b*-PCL copolymer seems to increase compatibility with matrix, improving dispersion of Fe<sub>2</sub>O<sub>3</sub> nanoparticles. For comparison, Figure 7 shows AFM image of nanocomposite with 5 wt% of unmodified nanoparticles. Bigger aggregates are formed, as nanoparticles tend to aggregate due to their low compatibility with the matrix. When Fe<sub>2</sub>O<sub>3</sub> nanoparticles are grafted with PMMA-*b*-PCL copolymer, they are mainly located at the interface between dark PCL and bright PS domains without breaking copolymer nanostructure. Size distribution of Fe<sub>2</sub>O<sub>3</sub>-*g*-(PMMA-*b*-PCL) in the nanocomposite annealed at 120 °C is shown in Figure 8 as an example. Average sizes of 22 and 38 nm are obtained for 2 and 5 wt% nanoparticle amount, respectively. Very similar results are obtained for those nanocomposites annealed at 100 °C. It has to be noted that the size of those aggregates is very similar to that obtained for Fe<sub>2</sub>O<sub>3</sub>-*g*-(PMMA-*b*-PCL), suggesting that aggregates are formed mainly during modification.

## CONCLUSION

Fe<sub>2</sub>O<sub>3</sub> nanoparticles have been successfully functionalized, both by silanization and subsequent copolymer grafting, as was demonstrated by FTIR and TGA. This functionalization seems to increase compatibility with copolymer, leading to good nanoparticle dispersion in the nanocomposites, without altering nanostructure generated by block copolymer self-assembly. Nanoparticles are mainly located at the interface between both blocks. During functionalization process, nanoparticles tend to create small aggregates surrounded by a copolymeric core, as it was corroborated by TEM. Those small aggregates are very similar in size that those found in the nanocomposites,

suggesting that dispersion of modified nanoparticles in the copolymer is good, much better than that of unmodified ones.

## ACKNOWLEDGEMENT

Financial support from the Basque Country Government (Grupos Consolidados, IT-365-07, Saiotek 2013 NANOSOL) and the Ministry of Education and Innovation (MAT 2012-31675) is gratefully acknowledged. I.B. thanks Euskal Herriko Unibertsitatea/Universidad del País Vasco for Ph.D Fellowship (Becas de Formación de Investigadores 2011 (PIF/UPV/11/030)).

## REFERENCES

- [1] Stasiaka, J., Nair, S., Moggridge, G.D. Mechanical strength of sutured block copolymers films for load bearing medical applications. *Bio-Medical Materials and Engineering* 2014, 24, 563-569. DOI:10.3233/BME-130843
- [2] Endres, T., Zheng, M., Kılıç, A., Turowska, A., Beck-Broichsitter, M., Renz, H., Merkel, O.M., Kissel T. Amphiphilic Biodegradable PEG-PCL-PEI Triblock Copolymers for FRET-Capable *in Vitro* and *in Vivo* Delivery of siRNA and Quantum Dots. *Molecular Pharmaceutics* 2014. DOI: 10.1021/mp400744a.
- [3] Jia, F., Zhang, Y., Narasimhan, B., Mallapragada, S.K. Block Copolymer-Quantum Dot Micelles for Multienzyme Colocalization. *Langmuir* 2012, 28, 17389-17395. DOI: 10.1021/la303115t
- [4] Shim, J.W., Kim, S.-H., Jeon, S.-J., Yang, S.-M., Yi, G.-R. Microcapsules with Tailored Nanostructures by Microphase Separation of Block Copolymers. *Chem. Mater.* 2010, 22, 5593-5600. DOI:10.1021/cm101696t
- [5] García, I., Tercjak, A., Gutierrez, J., Rueda, L., Mondragon, I. Nanostructuring via Solvent Vapor Exposure of Poly(2-vinyl pyridine-*b*-methyl methacrylate) Nanocomposites Using Modified Magnetic Nanoparticles. *J. Phys. Chem.* 2008, 112, 14343-14347. DOI: 10.1021/jp802345q
- [6] Gutierrez, J., Tercjak, A., Garcia, I., Mondragon, I. The effect of thermal and vapor annealing treatments on the self-assembly of TiO<sub>2</sub>/PS-*b*-PMMA nanocomposites generated via the sol-gel process. *Nanotechnology* 2009, 20, 225603. DOI:10.1088/0957-4484/20/22/225603



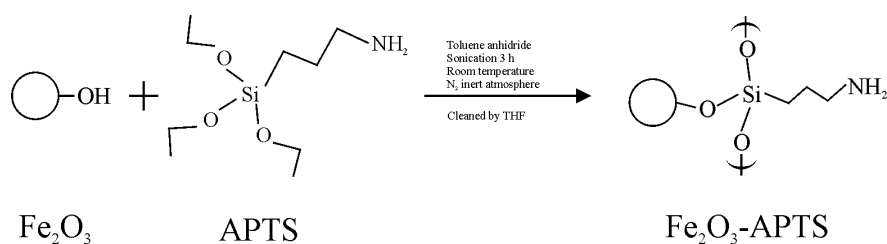
- [7] Etxeberria, H., Zalakain, I., Fernandez, R., Kortaberria, G., Mondragon, I. Controlled placement of polystyrene-grafted CdSe nanoparticles in self-assembled block copolymers. *Colloid Polym Sci* 2013, 291, 633-640. DOI: 10.1007/s00396-012-2765-0
- [8] Lopes, W.A., Jaeger, H.M. Hierarchical self-assembly of metal nanostructures on diblock copolymer scaffolds. *Nature* 2001, 414, 735-738. DOI:10.1038/414735a
- [9] Cheng, J.Y., Ross, C.A., Chan, V.Z-H., Thomas, E.L., Lammertink, R.G.H., Vancso, G.J. Formation of a Cobalt Magnetic Dot Array via Block Copolymer Lithography. *Adv. Mater.* 2001, 13, 1174-1178. DOI: 0935-9648/01/1508-1174
- [10] Ouk Kim, S., Solak, H.H., Stoykovich, M.P., Ferrier, N.J., de Pablo, J.J., Nealey, P.F. Epitaxial self-assembly of block copolymers on lithographically defined nanopatterned substrates. *Nature* 2003, 424, 411-414. DOI: 10.1038/nature01775
- [11] García, I., Zafeiropoulos, N.E., Janke, A., Tercjak, A., Eceiza, A., Stamm, M., Mondragon, I. Functionalization of Iron Oxide Magnetic Nanoparticles with Poly(methyl methacrylate) Brushes Via Grafting-From Atom Transfer Radical Polymerization. *Journal of Polymer Science: Part A: Polymer Chemistry* 2007, 45, 925-932. DOI: 10.1002/pola.21854
- [12] Kondo, A., Fukuda, H. Preparation of thermo-sensitive magnetic microspheres and their application to bioprocesses. *Colloids Surf A* 1999, 155, 435-438. DOI: S0927-7757(98)00465-8
- [13] Hsiao, J., Taic, M., Leed, Y., Yanga, C., Wangd, H., Liua, H., Fange, J., Chenf, S.J. Labelling of cultured macrophages with novel magnetic nanoparticles. *Magn Magn Mater* 2006, 304, e4-e6. DOI: 10.1016/j.jmmm.2006.01.134
- [14] Shen, H., Long, D., Zhu, L., Li, X., Dong, Y., Jia, N., Zhou, H., Xin, X., Sun, Y. Magnetic force microscopy analysis of apoptosis of HL-60 cells induced by complex of antisense oligonucleotides and magnetic nanoparticles. *Biophys Chem* 2006, 122, 1-4. DOI: 10.1016/j.bpc.2006.01.003
- [15] Peponi, L., Tercjak, A., Torre, L., Kenny, J. M., Mondragon, I. Surfactant Effects on Morphology-Properties Relationships of Silver-poly(styrene-b-isoprene-b-styrene)

Block Copolymer Nanocomposites *J Nanosci Nanotech* 2009, 9, 2128-2139. DOI: 10.1166/jnn.2009.437

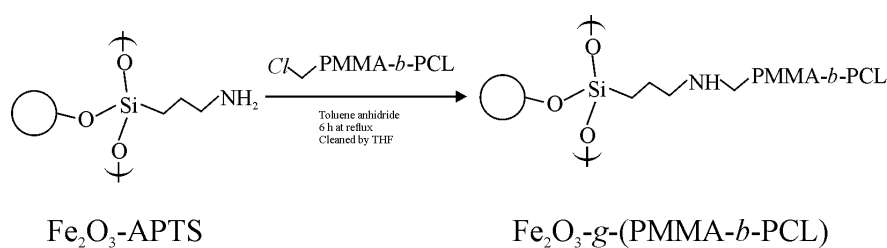
- [16] Etxeberria, H., Zalakain, I., Mondragon, I., Eceiza, A., Kortaberria, G. Generation of nanocomposites based on polystyrene-grafted CdSe nanoparticles by grafting through and block copolymer. *Colloid Polym Sci* 2013, 291, 1881-1886. DOI: 10.1007/s00396-013-2927-8
- [17] Minko, S., Patil, S., Datsyuk, V., Simon, F., Eichhorn, K., Motornov, M., Usov, D., Tokarev, I., Stamm, M. Synthesis of Adaptive Polymer Brushes via "Grafting To" Approach from Melt. *Langmuir* 2002, 18, 289-296. DOI: 10.1021/la015637q
- [18] Trabelsi, S., Janke, A., Häßler, R., Zafeiropoulos, N.E., Stamm, M., Fornasieri, G., Bocchini, S., Rozes, L., Gerard, J.-F., Sanchez, C. Novel Organo-Functional Titanium-oxo-cluster-Based Hybrid Materials with Enhanced Thermomechanical and Thermal Properties *Macromolecules* 2002, 35, 4960-4967. DOI: 10.1021/ma0507239
- [19] Wang, S., Zhou, Y., Guan, W., Ding, B. One-step copolymerization modified magnetic nanoparticles via surface chain transfer free radical polymerization. *Applied Surface Science* 2008, 254, 5170-5174. DOI: 10.1016/j.apsusc.2008.02.021
- [20] Zhou, Y., Wang, S., Ding, B., Yang, Z. Modification of magnetite nanoparticles via surface-initiated atom transfer radical polymerization (ATRP). *Chemical Engineering Journal* 2008, 138, 578-585. DOI: 10.1016/j.cej.2007.07.030
- [21] He, X., Wu, X., Cai, X., Lin, S., Xie, M., Zhu, X., Yan, D. Functionalization of Magnetic Nanoparticles with Dendritic-Linear-Brush-Like Triblock Copolymers and Their Drug Release Properties. *Langmuir* 2012, 28, 11929-11938. DOI: 10.1021/la302546m
- [22] Abbound, M., Turner, M., Duguet, E., Fontanille, M. PMMA-based composite materials with reactive ceramic fillers. Part 1. Chemical modification and characterization of nanoparticles. *J Mater Chem* 1997, 7, 1527-1532. DOI: 10.1039/A700573C

- [23]Jing, Z. Preparation and magnetic properties of fibrous gamma iron oxide nanoparticles via nonaqueous medium. *Mater Lett* 2006, 60, 2217-2221. DOI: 10.1016/j.matlet.2005.12.109
- [24]Wang, C., Ro, S. Nanoparticle iron-titanium oxide aerogels. *Mater Chem Phys* 2007, 101, 41-48. DOI: 10.1016/j.matchemphys.2006.02.010
- [25]Marutani, E., Yamamoto, S., Ninjbadgar, T., Tjii, Y., Fukuda, T., Takano, M. Surface initiated atom transfer radical polymerization of methyl methacrylate on magnetic nanoparticles. *Polymer* 2004, 45, 2231-2235. DOI: 10.1016/j.polymer.2004.02.005
- [26]Cosio-Castañeda, C., Martinez-Garcia, R., Socolovsky, L.M. Synthesis of silanized maghemite nanoparticles onto reduced graphene sheets composites. *Solid State Sci* 2014, 30, 17-20. DOI: 10.1016/j.solidstatesciences.2014.02.004
- [27]Mueller, R., Kammler, H.K., Wegner, K., Pratsinis, S.E. OH Surface Density of SiO<sub>2</sub> and TiO<sub>2</sub> by Thermogravimetric Analysis. *Langmuir* 2003, 19, 160-165. DOI: 10.1021/la025785w
- [28]Galeotti, F., Bertini, F., Scavia, G., Bolognesi, A. A controlled approach to iron oxide nanoparticles functionalization for magnetic polymer brushes. *Journal of Colloid and Interface Science* 2011, 360, 540-547. DOI: 10.1016/j.jcis.2011.04.076
- [29]Rana, S., Yoo, H.J., Cho, J.W, Chun, B.C., Park, J.S. Functionalization of Multi-Walled Carbon Nanotubes with Poly( $\epsilon$ -caprolactone) Using Click Chemistry. *Journal of Applied Polymer Science* 2011, 119, 31-37. DOI: 10.1002/app.31268
- [30]Ferriol, M., Gentilhomme, A., Cochez, M., Oget, N., Mieloszynski, J.L. Thermal degradation of poly(methyl methacrylate) (PMMA): modelling of DTG and TG curves. *Polymer Degradation and Stability* 2003, 79, 271-281. DOI: 10.1016/S0141-3910(02)00291-4
- [31]Ohno, K., Koh, K., Tsuji, Y., Fukuda, T. Synthesis of gold nanoparticles coated with well-defined, high density polymer brushes by surface-initiated living radical polymerization. *Macromolecules* 2002, 35, 8989. DOI: 10.1021/ma0209491

## FIGURE AND SCHEME CAPTIONS



**Scheme 1.** Procedure used for  $\text{Fe}_2\text{O}_3$  nanoparticle silanization



**Scheme 2.** Procedure used for grafting the block copolymer to the nanoparticles surface

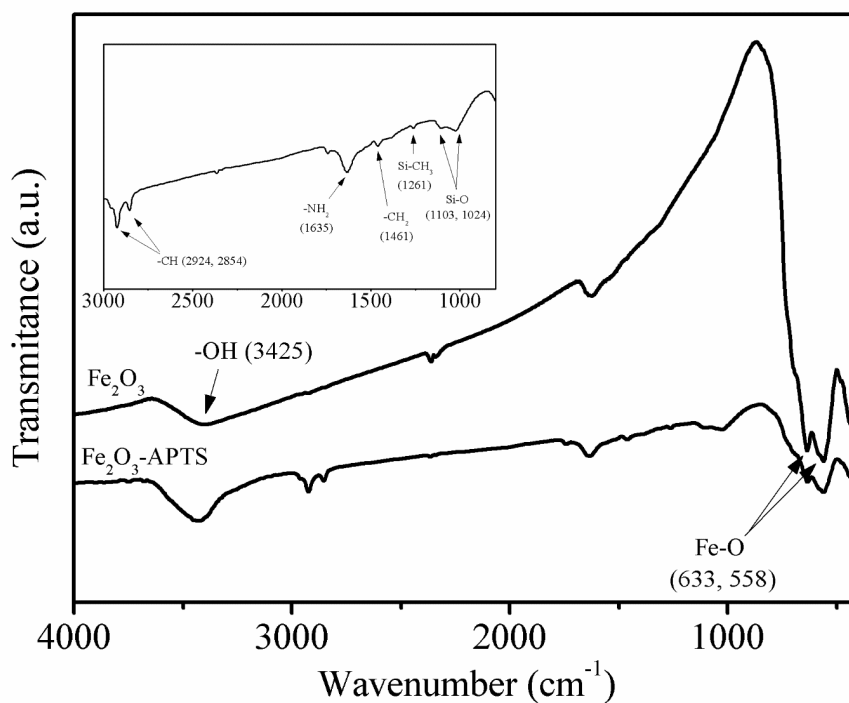


**Figure 1.** FTIR spectra of neat and silanized  $\text{Fe}_2\text{O}_3$  nanoparticles. Main bands are indicated by arrows. Inner spectrum shows a magnification of modified nanoparticle spectrum.

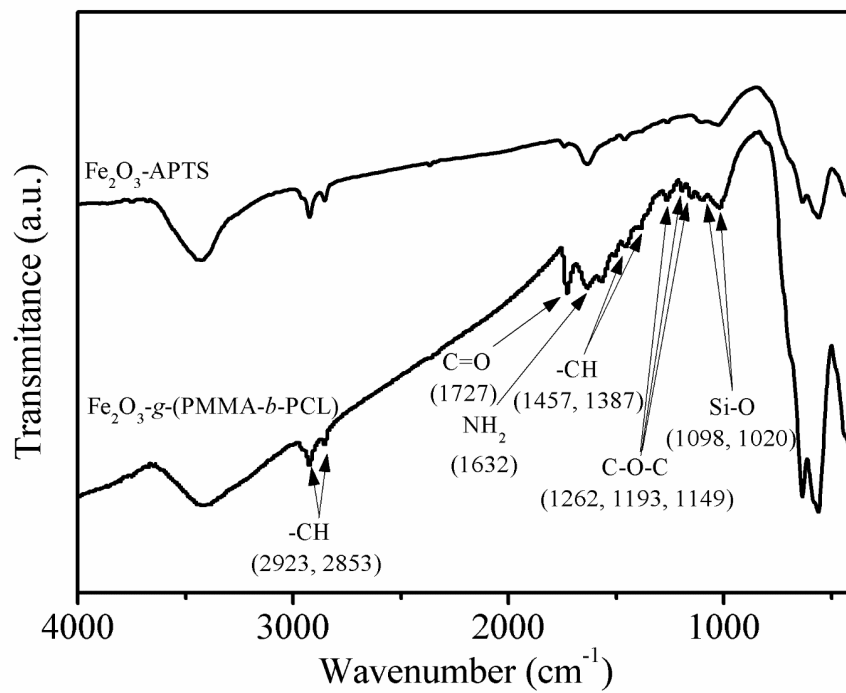


**Figure 2.** FTIR spectra of silanized and PMMA-*b*-PCL-grafted nanoparticles. Main bands are indicated by arrows.

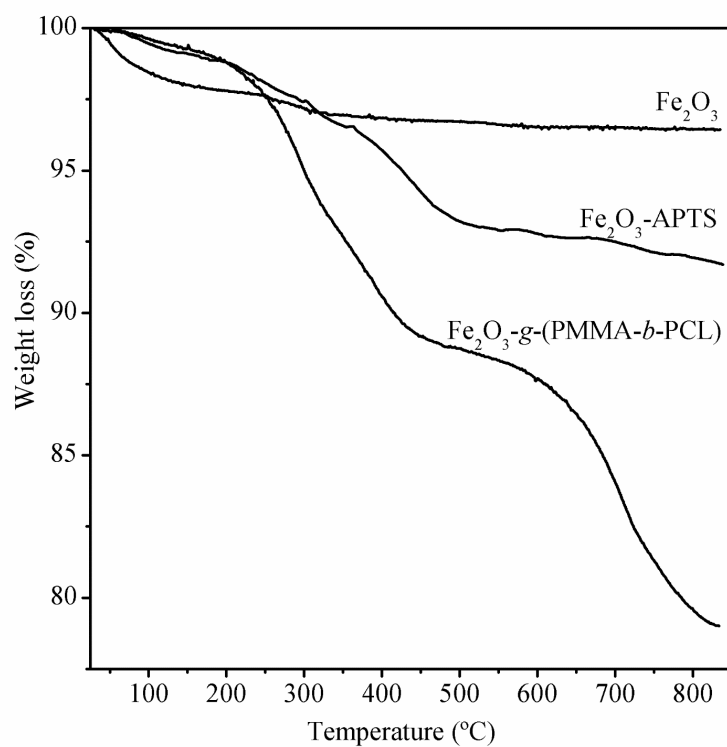


**Figure 3.** TGA thermograms of unmodified, silanized and grafted  $\text{Fe}_2\text{O}_3$  nanoparticles

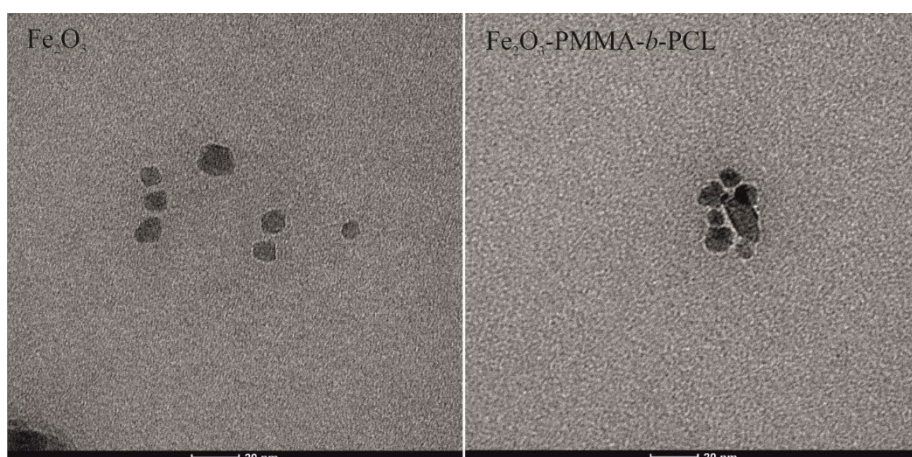


**Figure 4.** TEM images of modified and unmodified Fe<sub>2</sub>O<sub>3</sub> nanoparticles.

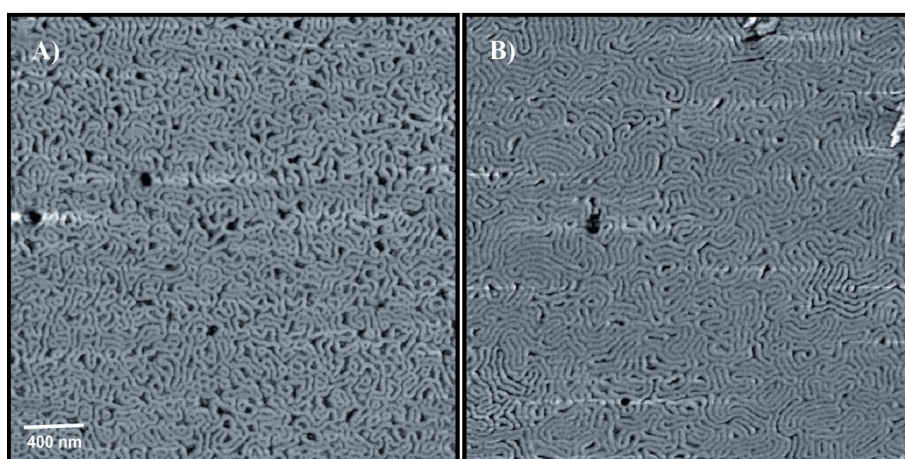


**Figure 5.** AFM phase images of PS-*b*-PCL block copolymer annealed for 72 h at: a) 100 °C, and b) 120 °C.

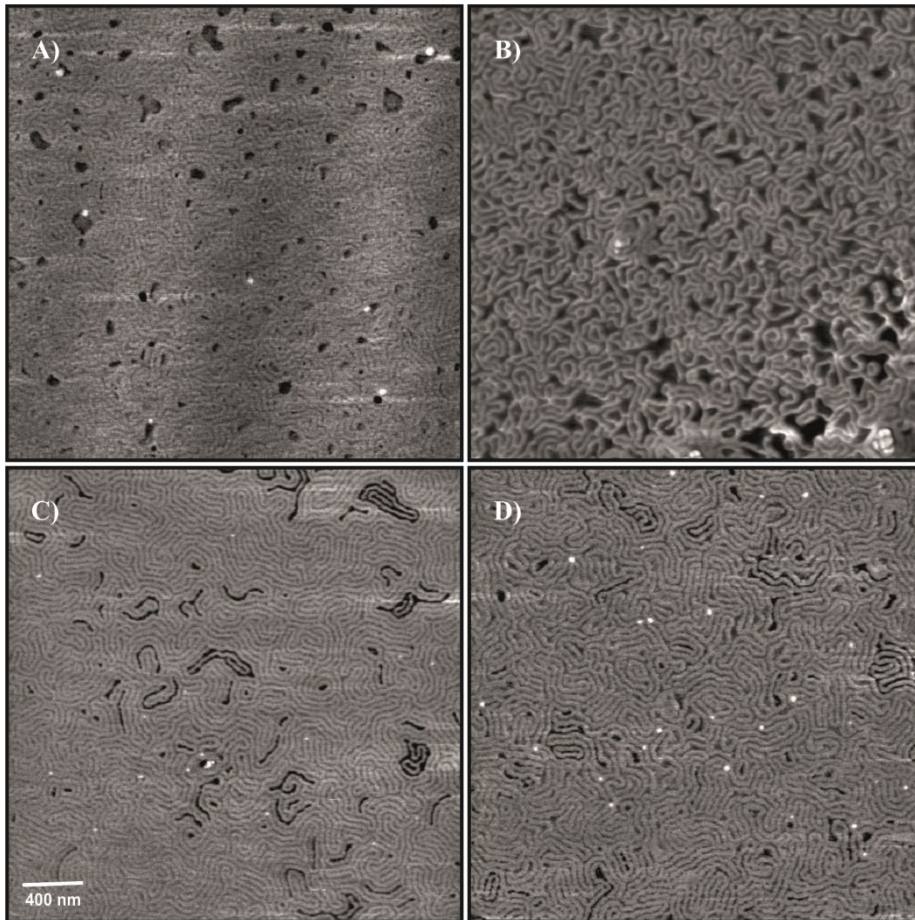


**Figure 6.** AFM phase images ( $3 \times 3 \mu\text{m}$ ) of PS-*b*-PCL/ $\text{Fe}_2\text{O}_3$ -g-(PMMA-*b*-PCL) nanocomposites annealed at different temperatures and nanoparticle amounts: a)  $100^\circ\text{C}$  and 2 wt%, b)  $100^\circ\text{C}$  and 5 wt%, c)  $120^\circ\text{C}$  and 2 wt% and d)  $120^\circ\text{C}$  and 5 wt%.

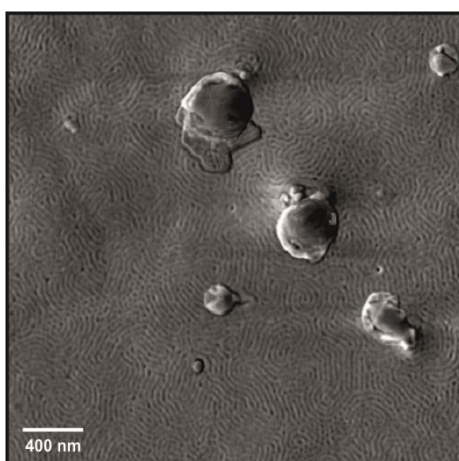


**Figure 7.** AFM phase image ( $3 \times 3 \mu\text{m}$ ) of PS-*b*-PCL/ $\text{Fe}_2\text{O}_3$  nanocomposites with 5 wt% of nanoparticles, annealed at  $120^\circ\text{C}$  for 72 h.

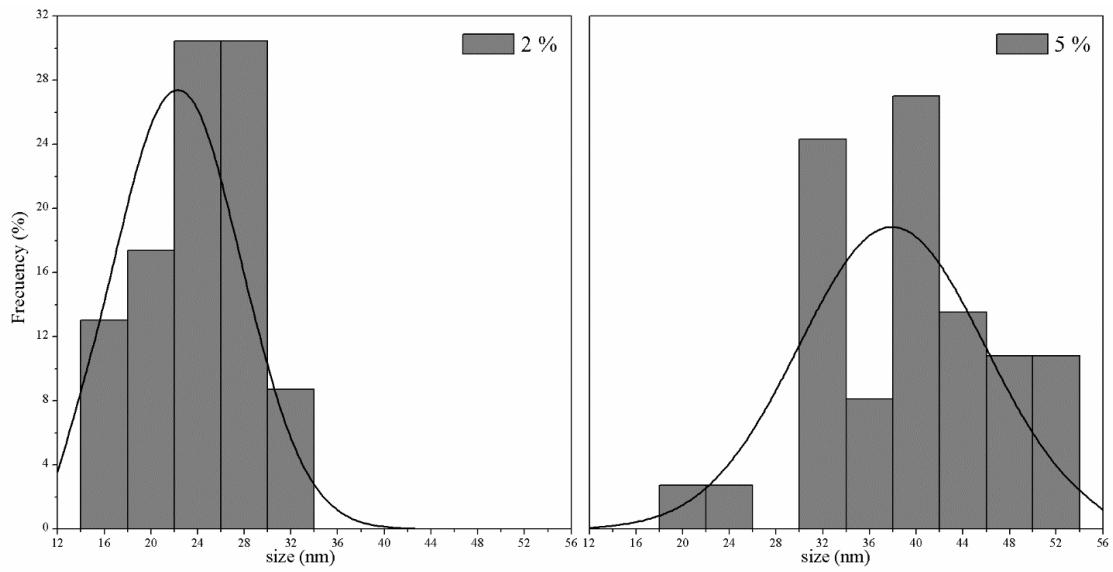


**Figure 8.**  $\text{Fe}_2\text{O}_3$ -g-(PMMA-*b*-PCL) size distribution in the nanocomposite annealed at 120 °C with: a) 2 wt% and b) 5 wt% of nanoparticles.